

Controlling the kinetic order of spin-reorientation transitions in Ni/Cu(100) films by tuning the substrate step structure

C. Klein,¹ R. Ramchal,² A. K. Schmid,^{1,*} and M. Farle²¹National Center for Electron Microscopy, Lawrence Berkeley National Laboratory, Berkeley, California 94720, USA²Fachbereich Physik, Universität Duisburg-Essen, 47048 Duisburg, Germany

(Received 8 March 2007; published 17 May 2007)

To study whether spin-reorientation transitions in 8–10 ML thick Ni/Cu(100) films take place by continuous or discontinuous rotation of the magnetization, we used spin-polarized low-energy electron microscopy to image the magnetization vector of magnetic domains during Ni growth. After substrate preparations that either promote or suppress bunching of atomic steps, we find strong evidence for either first- or second-order transition kinetics. The results are explained in terms of a magnetic phase diagram, taking the effect of topography on magnetic anisotropy contributions into account.

DOI: [10.1103/PhysRevB.75.193405](https://doi.org/10.1103/PhysRevB.75.193405)

PACS number(s): 68.37.Nq, 75.70.Ak, 34.80.Nz, 75.30.Gw

Phase transitions are among the most fundamental phenomena in condensed-matter physics. They proceed either discontinuously (first order) or continuously (higher order). In general, changing the kinetic order of a phase transition is possible only under very special circumstances, i.e., close to a critical point of the phase diagram. In magnetism such special systems have attracted attention before: Some metamagnetic antiferromagnets are known where temperature determines the order of the metamagnetic phase transition [e.g., FeCl₂ (Ref. 1)]. In this Brief Report, we introduce topology as a new critical parameter and show that the thickness-dependent spin-reorientation transition (SRT) in ultrathin Ni films grown on Cu(100) occurs close to a topology-driven critical point. The out-of-plane component of the magnetization changes either continuously over a thickness range of 0.6 ML equivalents or discontinuously within the experimental resolution ($\approx 1\%$ ML) depending on substrate morphology. Subtle manipulation of the arrangement of atomic steps on the Cu(100) substrate surface allows us to switch the kinetic order of this SRT between continuous and discontinuous changes of the magnetization direction.

SRTs are well known to occur in many ultrathin ferromagnetic films as a function of temperature or thickness.² Epitaxial Ni/Cu(100) films are particularly interesting because an inverse SRT from planar to perpendicular orientation of the magnetization is observed^{3–10} and the kinetic order of this transition is still under discussion.^{3–6} In this system, starting from in-plane magnetization of thinner Ni films, thickness-dependent first-order transitions are manifested by nucleation and growth of domains that are magnetized perpendicular to the film plane. In contrast, continuous variation of the polar angle of the magnetization vector (spin canting) indicates SRTs with kinetics of second order. Using spin-polarized low-energy electron microscopy (SPLEEM), we show that by minor modifications of the preparation procedure of the Cu substrate we can tune the intrinsic magnetic anisotropy energy (MAE) of the deposited Ni film to such extent that the kinetic order of the phase transition switches.

All experiments were performed in the SPLEEM at the Lawrence Berkeley National Laboratory at a base pressure below 5×10^{-11} mbar. The crystals were cleaned in the preparation chamber ($p \approx 10^{-10}$ mbar) by bombardment with

2 kV Ar ions while annealing the sample for 1 min in cycles repeated every 10 min. This automated preparation procedure was performed for many hours resulting in Auger-electron spectra, which show no contaminations. Figures 1(a) and 2(a) show LEEM images of clean Cu(100) substrates, highlighting how slightly different annealing temperatures can result in rather different surface topographies. Relatively high annealing temperature (1050 K), combined with moderate sputtering rate ($0.5 \mu\text{A}/\text{cm}^2$), promotes the bunching of atomic surface steps [Fig. 1(a)], yielding atomically flat terraces with micrometer dimensions. Through lower annealing temperature (850 K) step bunching can be suppressed [Fig. 2(a)], resulting in higher step densities. Ni films were deposited onto as-prepared surfaces *in situ* at 300 K by evaporation from an electron-beam evaporator.¹¹ The maximum pressure increase during film growth was below 1×10^{-10} mbar. Film thickness was controlled by monitoring the intensity oscillations of LEEM images taken during *in situ* film growth.^{12,13} The evaporation rate was typically about 0.15 ML/min. Together with our imaging rate of typically 15 frames/min this permits us to track the out-of-plane component of the film magnetization with up to 0.01 ML thickness resolution.

SPLEEM's sensitivity to topographic features such as atomic steps and step bunches¹⁴ and its capability to simultaneously record images showing magnetic contrast¹⁵ were exploited in order to correlate topography and magnetic domain formation during film growth (Figs. 1 and 2). Magnetic contrast in SPLEEM is proportional to the scalar product of the beam polarization and magnetization of the film. This dependence can be used to determine the local three-dimensional magnetization vector by evaluating the magnetic contrast in images obtained using three orthogonal polarizations of the incident beam.¹⁶ Therefore, as a function of Ni film thickness, we recorded triplets of SPLEEM images (at closed shutter) using beam polarization parallel to the surface normal and two orthogonal polarizations parallel to the film.

Room-temperature deposition of Ni films onto surfaces, which show pronounced step bunching, results in an onset of in-plane magnetic contrast around 5 ML, in agreement with previous investigations.^{3,18,19} Figure 1 summarizes SPLEEM

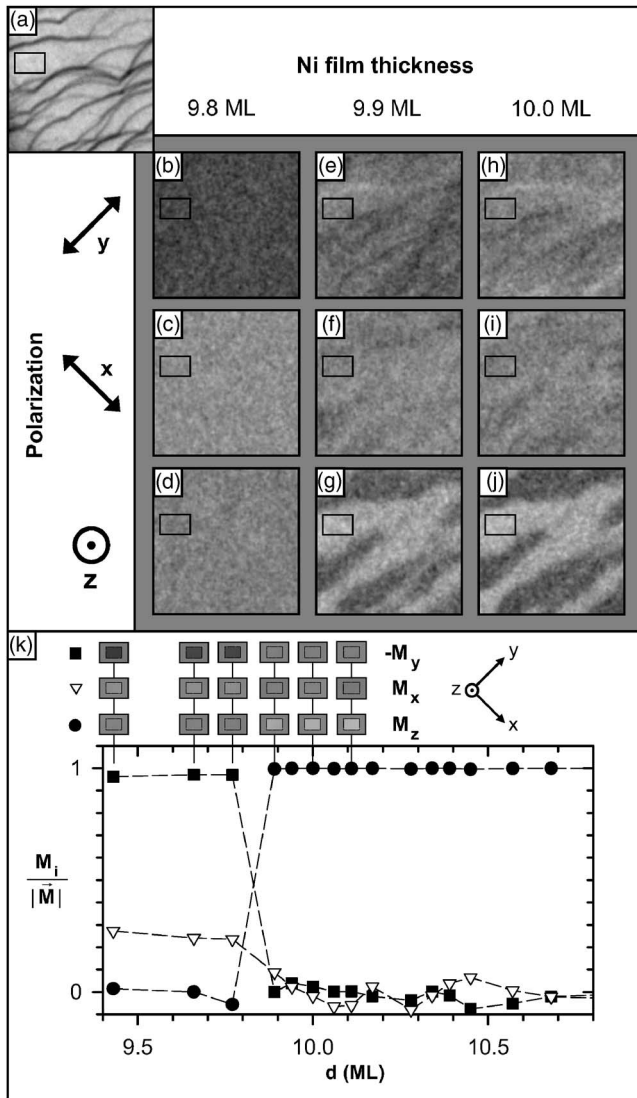


FIG. 1. SRT of first order in Ni/Cu(100) film grown on substrate showing pronounced step bunches. $2 \times 2 \mu\text{m}^2$ LEEM (a) and SPLEEM [(b)–(j)] images show topography and dependence of magnetic contrast on Ni/Cu(100) film thickness and polarization direction of illuminating electron beam (background gray level corresponds to null contrast). Dark contrast in (b), combined with null contrast in (d), indicates homogeneous in-plane magnetization. Strong bright and dark contrast in (g) and (j), combined with vanishing contrast in flat areas of (e), (f), (h), and (i) reveals abruptly formed, stripe-shaped, out-of-plane magnetized domains (Ref. 17). (k) Normalized xyz components of \vec{M} demonstrating the abruptness of the SRT. Rectangular insets show averaged gray and background levels of areas highlighted in (a)–(j).

observations of the SRT in films grown on this substrate morphology. Before the SRT, domain size is larger than the field of view ($7 \mu\text{m}$) and we do not observe an evident relationship between the magnetization direction and the average direction of the step bunches. Interestingly, at a critical thickness of 9.9 ML, the sudden formation of stripe domains magnetized perpendicular to the film is observed. On top of perfectly flat areas, the SRT is completed abruptly on the time scale of our measurements, with no indication of spin cant-

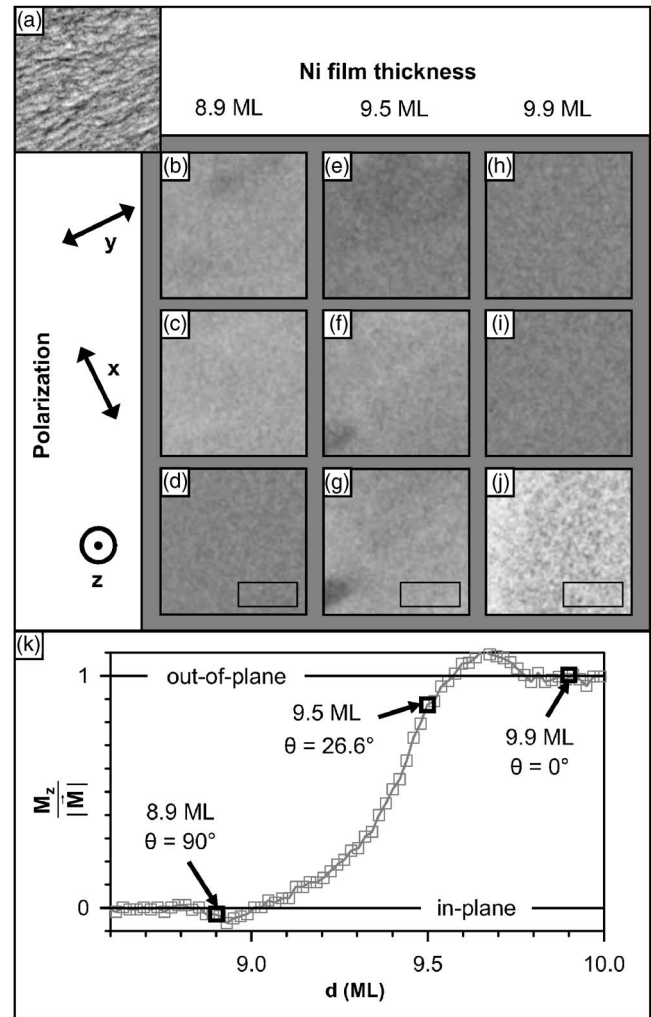


FIG. 2. SRT of second order in Ni/Cu(100) film grown on substrate showing no step bunches. $2 \times 2 \mu\text{m}^2$ LEEM (a) and SPLEEM [(b)–(j)] images show topography and dependence of magnetic contrast on Ni/Cu(100) film thickness and polarization direction of illuminating electron beam (background gray level corresponds to null contrast). As a result of continuous rotation of the magnetization from in plane to out of plane with increasing Ni thickness, magnetic contrast gradually increases for spin polarization along the surface normal (bottom row), while magnetic contrast fades for in-plane spin polarization (upper and middle rows). (k) Normalized out-of-plane component of \vec{M} recorded during Ni deposition [separate experiment, black squares represent corresponding results for panels (d), (g), and (j)].

ing (see black rectangles in Fig. 1). In other words, within the thickness resolution of our experiments, one additional Ni atom switches the orientation of several hundred film atoms. This is strong evidence of a first-order transition.

The behavior of the thickness-dependent SRT is considerably different when we use Cu(100) substrates where step bunching was suppressed. Although the onset of ferromagnetic order is again observed at ≈ 5 ML film thickness on these substrate surfaces, we always found the SRT to occur via continuous rotation of the magnetization. An example is summarized in Fig. 2. At Ni film thickness below the critical thickness where the SRT starts, we find again large in-plane

magnetized domains, the majority of which is oriented roughly perpendicular ($\pm 15^\circ$) to the average direction of the Cu steps [(b) and (c)]. When the Ni film thickness reaches 9.1 ML, the onset of magnetic contrast can be observed in images recorded with out-of-plane beam polarization. During deposition of an additional 0.5 ML Ni, magnetic contrast is visible for all three (orthogonal) SPLEEM images [see panels (e)–(g)], clearly indicating a canted magnetization vector. In this thickness range, the out-of-plane component of \vec{M} grows continuously until the magnetization is eventually oriented perpendicular to the film surface at 9.6 ML [panel (k)]. Consequently, the SRT for films grown on Cu(100) crystals which show no step bunching proceeds via continuous rotation of the magnetization vector. This is strong evidence for second-order transition kinetics.

The results show that surface topography of the Cu substrate considerably influences the SRT kinetics, allowing for the remarkable possibility that the Ni/Cu(100) SRT can be switched between first- and second-order phase transition kinetics.

One might have expected that the order of a phase transition is robust and not easily influenced by relatively subtle differences such as surface step structures. To understand how the remarkably different behaviors of otherwise similar films can result from different substrate topographies, one can consider the magnetization-dependent, anisotropic part of the free-energy density. For an ultrathin film of tetragonal symmetry, it is given as²⁰

$$f = -\bar{K}_2 \cos^2 \theta - \frac{1}{2} K_{4\perp} \cos^4 \theta - \frac{1}{8} K_{4\parallel} (3 + \cos 4\varphi) \sin^4 \theta, \quad (1)$$

where $\bar{K}_2 = K_2 - \frac{1}{2} \mu_0 M^2$ is the effective second-order anisotropy constant, including magnetocrystalline and dipolar effects, $K_{4\perp}$ and $K_{4\parallel}$ are the corresponding fourth-order anisotropy constants, and θ and φ are angles with respect to the surface normal and [001]. Here, each anisotropy coefficient consists of a volume contribution and a thickness-dependent surface contribution, i.e., $K_i = K_i^V + K_i^S/d$. All these coefficients are known for the Ni/Cu(100) system^{4,20,21} and the influence of $K_{4\perp}$ was found to be small. Thus, we can start by focusing on the thickness dependence of \bar{K}_2 and $K_{4\parallel}$. Following Jensen and Bennemann²² and Millev and Kirschner,²³ it is convenient to consider the \bar{K}_2 – $K_{4\parallel}$ phase diagram as shown in Fig. 3. Minimization of the free-energy density with respect to θ and φ results in three stable and one metastable regions in the \bar{K}_2 – $K_{4\parallel}$ plane. In the left-hand, horizontally hatched region of Fig. 3, magnetization parallel to the film surface is the only stable configuration. In the right-hand, vertically hatched region, magnetization is perpendicularly oriented. The cross-hatched area in between represents a metastable phase, where both in-plane and out-of-plane orientations of the magnetization represent a local energy minimum. For negative $K_{4\parallel}$, however, in-plane (left) and perpendicular (right) phases are separated by another stable phase, where \vec{M} is tilted with respect to the surface normal. Jensen and Bennemann²² pointed out how transition kinetics

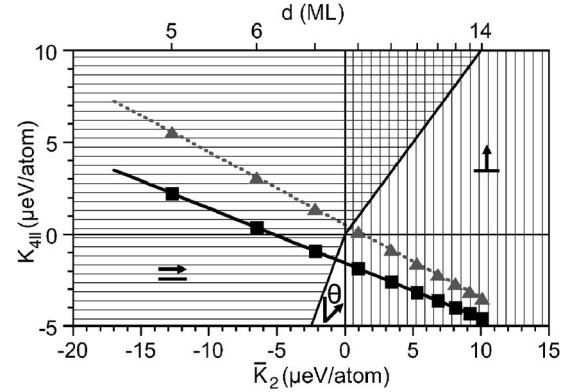


FIG. 3. Phase diagram for Ni/Cu(100) films. Square symbols: thickness-dependent anisotropies using experimental values given in Ref. 21. Triangular symbols: same data, shifted upward by assuming topography-induced change of fourth-order surface anisotropy constant $K_{4\parallel}^S$ by $15 \mu\text{eV}/\text{atom}$. See text for details.

follow from thickness-dependent changes in this phase diagram. To discuss our specific case of Ni/Cu(100), square symbols plotted in Fig. 3 represent the thickness-dependent, experimental values of \bar{K}_2 and $K_{4\parallel}$ taken from Ref. 21. One sees that, as the Ni film thickness increases from 5 ML to 14 ML, \bar{K}_2 increases and $K_{4\parallel}$ decreases. The diagram indicates that in films with thicknesses below 7.3 ML, in-plane magnetization is the stable configuration, and in films with thicknesses above 7.8 ML perpendicular magnetization is stable.²⁴ In the interval between 7.3 ML and 7.8 ML, Ni/Cu(100) films are in the region where \vec{M} is tilted with respect to the surface normal. Consequently, one would expect to find that the thickness-dependent SRT takes place via continuous canting of the magnetization, i.e., a transition of second order.

Considering the different substrate topographies shown in Figs. 1(a) and 2(a), one might be tempted to attribute the different behaviors observed for Ni films grown on step-bunched Cu substrates to pronounced differences in an additional step-induced, uniaxial, in-plane anisotropy $K_{2\parallel}$ as introduced by Bovensiepen *et al.*²⁵ However, such a contribution could only explain the observed behavior if it considerably increased the value of \bar{K}_2 , causing the critical thickness of the SRT to decrease by >1 ML. While this and similar effects (due to sample roughness or adsorbates) are known to occur,^{8,26–32} a decrease of the critical thickness has never been observed in our experiments. This points to the importance of the surface terms of the fourth-order anisotropy. Heinrich *et al.*³² have pointed out that lateral inhomogeneities at interfaces can result in fourth-order terms which decrease the total energy. In our sign convention that would imply a positive contribution to the surface term of $K_{4\parallel}$, shifting the curve of Fig. 3 into the metastable region where SRT's are discontinuous phase transitions. It is expected that this effect grows stronger with increasing atomic terrace width,³² in good agreement with our findings. To illustrate the effect of surfaces where high step bunches (inhomogeneities) separate large, atomically flat terraces, we added $+15 \mu\text{eV}/\text{atom}$ to the measured values for $K_{4\parallel}^S$ taken from

Ref. 21 and replotted the shifted anisotropies using triangular symbols. Evidently, this reasonable correction is sufficient to place the system entirely outside the unhatched region where tilted magnetization is stable. As a function of increasing thickness, the stability of in-plane magnetization is followed abruptly by stability of perpendicular magnetization; i.e., canted magnetization is unstable at all thicknesses. This is consistent with a SRT with first-order kinetics, as we observe when we grow Ni films on Cu(100) substrates with pronounced step bunching. We suggest that this is the mechanism that governs the switching between continuous and discontinuous SRTs we observe in ultrathin Ni/Cu(100) films.

In summary, the influence of substrate topography on the SRT of ultrathin Ni films grown on Cu(100) was studied by SPLEEM. For Cu crystals, which show no step bunching, a second-order SRT was observed, i.e., continuous rotation of the magnetization vector from in plane to out of plane. In contrast, on Cu substrates which show pronounced step

bunches, a discontinuous, first-order SRT was found to take place. This evidence for the occurrence of both transition kinetics on the same substrate reconciles discrepancies found in literature^{3-5,7} and might very well apply to other epitaxial systems as well [see, e.g., Co/Au(111) (Ref. 33)]. We attribute these different behaviors to changes of the MAE induced by the topography of the substrate and show that through controlled increase/decrease of surface step bunching, it is possible to switch back and forth between first- and second-order transitions in Ni/Cu(100).

ACKNOWLEDGMENTS

This work was sponsored by the Austrian Science Fund (J2352-N02), the Deutsche Forschungsgemeinschaft SFB 491, and the U.S. Department of Energy under Contract No. DE-AC02-05CH11231. We are grateful to J. Lindner for helpful discussions and for critical reading of the paper.

*Electronic address: akschmid@lbl.gov

¹S. Jacobs and P. E. Lawrence, Phys. Rev. **164**, 866 (1967).

²*Ultrathin Magnetic Structures I*, edited by J. A. C. Bland and B. Heinrich (Springer, Berlin, 1994).

³W. L. O'Brien and B. P. Tonner, Phys. Rev. B **49**, 15370 (1994).

⁴M. Farle, B. Mirwald-Schulz, A. N. Anisimov, W. Platow, and K. Baberschke, Phys. Rev. B **55**, 3708 (1997).

⁵M. Farle, W. Platow, A. N. Anisimov, P. Pouloupoulos, and K. Baberschke, Phys. Rev. B **56**, 5100 (1997).

⁶V. Jähnke, J. Gütde, and E. Matthias, J. Magn. Magn. Mater. **237**, 69 (2001).

⁷S. S. Dhesi, H. A. Dürr, and G. van der Laan, Phys. Rev. B **59**, 8408 (1999).

⁸R. Vollmer, T. Gutjahr-Loser, J. Kirschner, S. van Dijken, and B. Poelsema, Phys. Rev. B **60**, 6277 (1999).

⁹H. Fritzsche, J. Kohlhepp, H. J. Elmers, and U. Gradmann, Phys. Rev. B **49**, 15665 (1994).

¹⁰A. Hucht and K. D. Usadel, J. Magn. Magn. Mater. **198-199**, 493 (1999).

¹¹W. Platow, U. Bovensiepen, P. Pouloupoulos, M. Farle, K. Baberschke, L. Hammer, S. Waller, S. Müller, S. Müller, and K. Heinz, Phys. Rev. B **59**, 12641 (1999).

¹²C. M. Schneider, A. K. Schmid, H. P. Oepen, and J. Kirschner, *Magnetism and Structure in Systems of Reduced Dimension*, edited by R. F. C. Farrow, B. Dieny, M. Donath, A. Fert, and B. D. Hermsmeier (Plenum, New York 1993), pp. 453-466.

¹³K. L. Man, W. L. Ling, S. Y. Paik, H. Poppa, M. S. Altman, and Z. Q. Qiu, Phys. Rev. B **65**, 024409 (2001).

¹⁴M. S. Altman, W. F. Chung, and C. H. Liu, Surf. Rev. Lett. **5**, 1129 (1998).

¹⁵E. Bauer, T. Duden, and R. Zdyb, J. Phys. D **35**, 2327 (2002).

¹⁶R. Ramchal, A. K. Schmid, M. Farle, and H. Poppa, Phys. Rev. B **69**, 214401 (2004).

¹⁷Weak in-plane contrast can be discerned in Figs. 1(e), 1(f), 1(h), and 1(i). Comparison with panel (a) reveals that this contrast is

always associated with domain walls or pronounced step bunches.

¹⁸R. Ramchal, A. K. Schmid, M. Farle, and H. Poppa, Phys. Rev. B **68**, 054418 (2003).

¹⁹K. Baberschke, Appl. Phys. A: Mater. Sci. Process. **62**, 417 (1996).

²⁰B. Schulz and K. Baberschke, Phys. Rev. B **50**, 13467 (1994).

²¹M. Farle, Rep. Prog. Phys. **61**, 755 (1998).

²²P. J. Jensen and K. H. Bennemann, Phys. Rev. B **52**, 16012 (1995).

²³Y. Millev and J. Kirschner, Phys. Rev. B **54**, 4137 (1996).

²⁴Lower critical thickness is most likely caused by contamination from the residual gas phase (cf. influence of H₂ and O₂ adsorption as discussed in Refs. 25 and 27).

²⁵U. Bovensiepen, Hyuk J. Choi, and Z. Q. Qiu, Phys. Rev. B **61**, 3235 (2000).

²⁶J. Lindner, P. Pouloupoulos, R. Nýntheil, E. Kosubek, H. Wende, and K. Baberschke, Surf. Sci. **523**, L65 (2003).

²⁷A. B. Shick, Yu. N. Gornostyrev, and A. J. Freeman, Phys. Rev. B **60**, 3029 (1999).

²⁸D. Sander W. Pan, S. Ouazi, J. Kirschner, W. Meyer, M. Krause, S. Müller, L. Hammer, and K. Heinz, Phys. Rev. Lett. **93**, 247203 (2004).

²⁹P. Bruno, J. Appl. Phys. **64**, 3153 (1988).

³⁰C. Chappert and P. Bruno, J. Appl. Phys. **64**, 5736 (1988).

³¹P. Pouloupoulos, J. Lindner, M. Farle, and K. Baberschke, Surf. Sci. **437**, 277 (1999).

³²B. Heinrich, T. Monchesky and R. Urban, J. Magn. Magn. Mater. **236**, 339 (2001).

³³R. Allenspach, M. Stampanoni, and A. Bischof, Phys. Rev. Lett. **65**, 3344 (1990); H. P. Oepen, M. Speckmann, Y. Millev, and J. Kirschner, Phys. Rev. B **55**, 2752 (1997); H. F. Ding, S. Putter, H. P. Oepen, and J. Kirschner, Phys. Rev. B **63**, 134425 (2001).